# EurJIC

European Journal of Inorganic Chemistry

**Chemistry Europe**

European Chemical Societies Publishing

## Accepted Article

**Title:** Comparative Assessment of ESI-MS Softness for Inorganic Complexes: How Soft is Your ESI-MS?

**Authors:** Ian C. Chagunda, Peter J. H. Williams, Tiago Fisher, Naomi L. Stock, Daniel G. Beach, Gilian T. Thomas, Jane Zhu, and J. Scott McIndoe

**WILEY**▪VCH

# RESEARCH ARTICLE

# Comparative Assessment of ESI-MS Softness for Inorganic Complexes: How Soft Is Your ESI-MS?

Ian C. Chagunda,*[a] Peter J. H. Williams,[a] Tiago Fisher,[a] Naomi L. Stock,[b] Daniel G. Beach,[c] Gilian T. Thomas,[d] Jane Zhu,[e] and J. Scott McIndoe*[a]

[a] Ian C. Chagunda,* Dr. Peter J. H. Williams, Tiago Fisher, Dr. J. Scott McIndoe*
Department of Chemistry
University of Victoria
PO Box 1700 STN CSC, Victoria, BC V8W 2Y2, Canada
E-mail: chagunda@uvic.ca; mcindoe@uvic.ca

[b] Dr. Naomi L. Stock
Water Quality Centre
Trent University
1600 West Bank Drive, Peterborough, ON K9L 0G2, Canada

[c] Dr. Daniel G. Beach
Biotoxin Metrology
National Research Council Canada
1411 Oxford St., Halifax, NS B3H 3Z1, Canada

[d] Dr. Gilian T. Thomas
Centre for Catalysis Research and Innovation
Department of Chemistry and Biomolecular Sciences
University of Ottawa
10 Marie Curie, Ottawa, ON K1N 6N5, Canada

[e] Jane Zhu
Department of Chemistry
University of British Columbia
2036 Main Mall, Vancouver, BC V6T 1Z1, Canada

Supporting information for this article is given via a link at the end of the document.

**Abstract:** Electrospray ionization mass spectrometry (ESI-MS) is a powerful tool for identifying and characterizing organometallic and coordination compounds. However, detection of fragile structures bound by weaker intermolecular forces can be significantly limited in ESI-MS owing to the use of relatively harsh instrument conditions and configurations. In this study, a set of tests was developed to assess the softness of ESI-MS systems. Two variants are presented: positive ion mode, utilizing a mixture of sodium ions and triphenylphosphine oxide producing $[Na(OPPh_3)_n]^+$ ions ($n$ = 1-4), and negative ion mode utilizing $Pd(PPh_3)_4$ and sulfonated triphenylphosphine producing $[Pd(L)(PPh_3)_n]^-$ ions ($n$ = 0-2), where softer instrument conditions preserve a higher proportion of the high-coordinate ions and harsher conditions will result in increased detection of products of ion fragmentation. The results revealed notable variations in instrument softness, which were influenced by a combination of instrument design and experimental parameters. Meticulously optimizing experimental conditions and ESI-MS parameters is essential to achieving the softest ionization possible, ensuring reliable analysis where applicable. This study offers valuable insight through straightforward tests that can be employed to assess the suitability of an instrument for specific research needs.

## Introduction

Mass spectrometry (MS) is an indispensable analytical tool in chemistry and other natural sciences. In the field of organometallic chemistry, electrospray ionization (ESI) MS has emerged as a powerful tool to identify and characterize new compounds, study reaction mechanisms and dynamics, and establish speciation in complex mixtures.[1–8] As a soft ionization technique, ESI is noted for producing ions with minimal fragmentation, making it highly suitable for thermally fragile species that are not amenable to other ionization techniques, such as electron ionization.[9] Despite the soft character of the ESI process, it is not immune to ion fragmentation and aggregation, which can complicate spectral interpretation and peak recognition, thus compromising analysis.[10]

The behavior and extent of fragmentation of ions is closely tied to the internal energy acquired during the ionization process, which encompasses the total energy above the ions' electronic, vibrational, and rotational ground states. The dissociation rate is influenced by both the internal energy as well as the timescale of the experiment, equal to the ion flight time between the source and the mass analyzer.[11,12] It is important to differentiate between the internal energy and the kinetic energy in ions, as conversion of kinetic energy to internal energy plays a significant role in

# RESEARCH ARTICLE

influencing ion behavior and fragmentation outcomes. This conversion can be modelled by two energy transfer mechanisms: (1) the formation of long-lived complexes between the ion and background gas, leading to energy redistribution into internal energy and relative translation energy upon dissociation; and (2) the impulsive collision mechanisms where vibrational energy is transferred from the recoil energy of inelastic collision.[11]

Additionally, as ions or charged droplets are subjected to rapid decrease in pressure during their transition from the atmospheric pressure source into the high vacuum region of the mass analyzer ($10^{-3}$ to $10^{-10}$ Torr, depending on the type of analyzer), they can experience acceleration.[13] The axial velocity component is amplified as a result of supersonic expansion as ions and charged droplets pass through successive differential pumping stages separated by small orifices.[14] This acceleration and subsequent increased occurrence of collisions leads to an increase in the energy per particle, enhancing the likelihood of ion fragmentation.[11,15] Furthermore, acceleration by strong electric field gradients in the intermediate pressure regions intensifies the frequency of energetic collisions with residual background gases, thus promoting ion activation and fragmentation.[15–17]

Together, these aspects highlight the dynamic and multifaceted nature of in-source fragmentation and collision induced dissociation (CID) in ESI-MS, where factors such as collision dynamics, energy transfer mechanisms, and the nature of interactions between ions and their surroundings all play a pivotal role in ion dissociation. Design of the ionization source, MS interface and ion optics, the composition of the solvent used, and the instrument settings can all contribute to an ESI instrument's ionization efficiency and softness.[18–21] As a result, spectra from different instruments might vary significantly, making it challenging to compare and to reproduce ESI-MS spectra.

Several studies on instrument parameter optimization have been published. One such study delved into careful optimization of various parameters to enhance sampling efficiency, and suggested providing fixed optimal values for key source parameters to simplify ESI-MS.[22] Another investigation focused on the internal energy distribution of benzylammonium ions produced through secondary electrospray ionization (SESI), revealing the relatively harsh instrument settings commonly used for SESI, and highlighting the need for precise instrument tuning necessary to take advantage of its softness.[23] Additionally, the introduction of a new class of thermometer ions, benzhydrylpyridinium, has also offered a potential avenue for determining the internal energies of ions generated in ESI, with potential implications for optimization of instrument parameters for ESI-MS.[24]

Research conducted withing the McIndoe group focuses on investigating catalytic reactions with ESI-MS, particularly those characterized by weak interactions between organometallic metal complexes and substrates.[25–27] Understanding the mechanistic properties of such catalytic processes is essential for the development of new synthetic routes, the production of value-added commercial materials, and the promotion of chemical sustainability. However, facing challenges in obtaining consistent results is common due to substantial differences between ESI-MS instruments, reflecting the variety in specific instrument design. Recognizing the impact of these disparities is crucial and selecting the appropriate MS instrument and source is vital for

accurate detection of the species of interest. Therefore, addressing these challenges becomes paramount in improving the reproducibility and comparability of our findings.

To address this, we conducted a comparative assessment of ESI-MS instruments to evaluate their relative softness using a simple but sensitive experiment in both positive and negative ion mode. In this context, a source's "softness" is a qualitive measure of the minimum internal energy imparted to ions during ionization and subsequent transfer into the gas phase, while avoiding imparting extra internal energy post-ionization, which promotes fragmentation.[11] While the minimal energy required for ionization is largely determined by the ionization method and instrument design, the avoidance of additional energy transfer can be achieved by carefully adjusting experimental conditions and instrument parameters.

To validate our findings, we tested different ESI-MS instruments from various manufacturers, revealing substantial differences in instrument softness. This study therefore aims to provide simple tests that allow researchers to qualitatively probe the energetic conditions of their instrument, with a focus on of organometallic or inorganic chemists. It is important to note that these tests, unlike those developed using thermometer ions,[23,24,28] do not seek to provide a quantitative characterization of internal energies. Instead, they can serve as a straightforward method for assessing instrument softness, and as a practical tool for evaluating instrument suitability in detecting thermally fragile organometallic and coordination species.

## Results and Discussion

### Initial assessment of instrument softness for Systems 1 and 2

The positive ion mode test utilized triphenylphosphine oxide (OPPh$_3$) and sodium chloride, both cheap and readily available starting materials. Phosphine oxide is notable due to the considerable basicity of the oxygen atom, and its propensity to aggregate with charged species in solution.[29,30] Charged species can be formed through Brönsted–Lowry acid–base reactions, resulting in protonated molecules ($[M + H]^+$), or through the Lewis acid–base mechanism, which forms coordination complexes involving cations with neutral molecules (e.g., $[M + Na]^+$). Both the protonated and sodiated species are anticipated to be present in appreciable concentrations within the bulk solution,[31] despite binding constants in ESI-MS being reported to be on average two orders of magnitude larger than those detected in solution.[32] When OPPh$_3$ is sodiated, the resulting spectra appear uncomplicated, with $[Na(OPPh_3)_n]^+$ and a maximum of four coordinated ligands.[33] The $n = 4$ species emerges as the most diagnostic peak, appearing prominently in some instruments while being entirely absent in others.

Two mass spectrometers were used in the initial stages of method development: the Waters Tandem Quadrupole Detector (TQD) spectrometer (System 1) and the Waters Synapt G2-S*i* QuanTof ESI-ion mobility spectrometry-MS (ESI-IMS-MS) spectrometer (System 2). The instrument source parameters were not initially optimized, with settings based on values recommended by the manufacturer. Parameters were then optimized to minimize ion fragmentation using OptiMS,[34] with the parameter details

# RESEARCH ARTICLE

provided in Tables S1 and S2 of the Supporting Information (SI). Both instruments were equipped with an atmospheric-pressure ionization (API) source, where differential pumping transfers ions from ambient pressure into the high vacuum of a mass analyzer.[13]

In System 1, samples are introduced into the ionization source, pass through the sample cone into the vacuum system, and proceed to the first quadrupole for mass filtering based on the mass-to-charge ratio ($m/z$). The ion beam proceeds to the T-Wave collision cell for CID or additional $m/z$ filtering in the second quadrupole.[35] In contrast, System 2 directs samples through a sampling orifice in the ionization source, then via StepWave transfer optics with a narrow bore ion guide to eliminate neutral species. The ion beam is filtered by quadrupole, passes through the TriWave region with T-Wave ion guides for ion trapping, accumulation, release, and transfer to the time-of-flight (TOF) analyzer.[36] Additionally, the second T-Wave can function as an ion mobility separator.
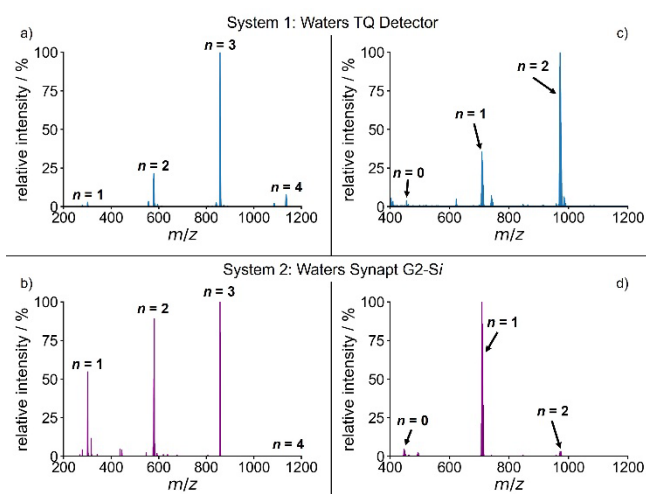


**Figure 1.** Left: Positive-ion ESI mass spectra for Systems 1 (a) and 2 (b) collected at 120 °C and 80 °C source temperatures, respectively. Samples consist of 0.05 mM and 0.2 mM NaCl and OPPh$_3$, respectively, producing [Na(OPPh$_3$)$_n$]$^+$ ions, where n = 1-4. The 100% relative intensity represents 3.5 × 10$^6$ cps. and 2.2 × 10$^9$ cps. absolute ion intensities for (a) and (b), respectively. Right: Negative-ion ESI mass spectra for Systems 1 (c) and 2 (d), collected at 100 °C source temperatures. Samples consist of 0.5 mM Pd(PPh$_3$)$_4$ and [PPN]$^+$[P(Ph)$_2$(m-C$_6$H$_4$SO$_3$)]$^-$ or [PPN][1], producing [Pd(1)(PPh$_3$)$_n$]$^-$ ions, where n = 0-2. The 100% relative intensity represents 2.6 × 10$^5$ cps. and 1.8 × 10$^9$ cps. absolute ion intensities for (c) and (d), respectively.

Figure 1 shows mass spectra collected from the two initial ESI-MS test instruments in positive ion mode, using their non-optimized instrument parameters. The strongest relative signal intensity for the n = 4 ion peak was observed in System 1 (Figure 1a). The intensities of the observed peaks varied as anticipated, depending on the metal-ligand mole ratio used in sample preparation. The best signal intensity for the tetrakis cation [Na(OPPh$_3$)$_4$]$^+$ is obtained with a 1:4 mole ratio of sodium ions to triphenylphosphine oxide (additional details on variable stoichiometry for System 1 can be found in the SI.

The tetrakis cation [Na(OPPh$_3$)$_4$]$^+$ was detected with minimal signal intensity in System 2 (Figure 1b). Its absolute intensity was 1.2 × 10$^6$ counts per second (cps.), which was three orders of magnitude less than the intensity of the n = 3 species, which was 2.2 × 10$^9$ cps. This low n = 4 signal intensity did not register significantly above the background noise level of 2.4 × 10$^5$ cps., even when excess OPPh$_3$ was added to the sample. This observation may not be attributed solely to in-source fragmentation, but rather to be a known effect of the instrument design. As a hybrid ESI-IMS-MS instrument, ions must pass through the IMS drift tube, regardless of whether IMS experiments are being undertaken, extending the experiment's timescale. This extended duration of transients may promote an increase in the frequency of energetic ion collisions with background drift gas molecules, resulting in greater ion internal energy and promoting fragmentation.[37] Furthermore, recent investigations into structural rearrangements in trapped ion mobility spectrometry (TIMS) revealed that the effective vibrational temperature of ions inside the TIMS tunnel exceeds 500 K.[38] This suggests that a similar phenomenon is likely at play in System 2, where the upstream effective vibrational temperature of ions likely exceeds the source temperature.

In negative ion mode, a parallel test was employed. In this case, we combined Pd(PPh$_3$)$_4$ and sulfonated triphenylphosphine, [1]$^-$, generating a series of [Pd(1)(PPh$_3$)$_n$]$^-$ ions, where n = 0-2. Given that Pd(PPh$_3$)$_4$ primarily exists in solution as the trisligated Pd(PPh$_3$)$_3$ species formed following ligand dissociation,[39] the introduction of a charge-tagged analogue of PPh$_3$ facilitates the generation of anionic species through ligand exchange, making the complex detectable in negative mode ESI-MS. Previous work has demonstrated the utility of charge-tagged analogues in illuminating reaction intermediates in ESI-MS studies, with their reactivity closely mirroring that of their neutral analogues.[40–42] In this context, detection of the n = 2 trisligated ion implies preservation of weaker metal-ligand interactions in a "softer" source.

Similar trends to those observed in positive ion mode were also evident in the negative ion mode. System 1 produced the best results, prominently featuring the diagnostic n = 2 ion peak (Figure 1c). In contrast, System 2 produced distinct spectra characterized by a higher relative abundance of the n = 1 species with less than 5% relative abundance of the n = 2 ion peak (Figure 1d). The increased prevalence of the monophosphine ion, [Pd(1)]$^-$, for System 2 can be attributed to ion fragmentation, as high concentrations of this species are not accessible in solution.[43] These findings track closely with the observations from the positive mode test, where extensive fragmentation of the most fragile species occurred, likely due to additional energy imparted within the drift tube. The obtained data highlighted the spectral variability initially observed for both systems.

## Enhancing softness through automated optimization of instrument parameters

To address the range of findings obtained from the two test instruments, we investigated how optimizing instrument parameters might enhance softness. To get ideal spectral data, substantial parameter optimization is required, as suboptimal settings used during characterization can negatively impact the

3

# RESEARCH ARTICLE

quality of results.[22] The difficulty of optimizing instrument parameters for unknown samples is recognized in real-world applications since it is frequently impossible to predict the precise characteristics of a new sample. However, we propose that the tests outlined in this study can facilitate the initial parameters optimization process for new sample analyses. By focusing on achieving softer ionization conditions that enhance the relative abundance of highly coordinated ions, researchers can establish a favorable starting point for tuning instrument parameters. This proactive approach offers a pathway to move away from default instrument settings, which may be too harsh for fragile species, towards conditions that maximize the detection of thermally fragile compounds.

Identifying optimal parameters can be time consuming and complex, made more difficult by the fact that optimizing one parameter may deoptimize another.[44] To address this, a semi-systematic optimization of the instrument parameters was conducted using OptiMS.[34] This Bayesian optimization method used a multivariate approach to first randomly sample across the search space defined by the chosen parameters, followed by subsequent optimization for highest signal intensity. Here, parameters were optimized for "softness" as defined by converging on a set of parameters that maximized the signal intensity of the $[Na(OPPh_3)_4]^+$ ($m/z \sim 1135.33$) or $[Pd(\mathbf{1})(PPh_3)_2]^-$ ($m/z \sim 971.13$) corresponding peaks.

The open-source OptiMS software not only streamlined the process but also allowed for automated systematic exploration of various parameter settings. This enabled efficient identification of optimal conditions for System 1, which involved reducing capillary and cone voltages to 1.5 kV and 10 V, respectively in positive mode, from their default settings of 4 kV and 30 V (details of optimized instrument parameters are summarized in the SI Table S1). Optimizing instrument conditions led to notable improvements in softness, exemplified by the enhanced relative intensity achieved across all ions, including the diagnostic $n = 4$ species, as well as an absolute signal intensity increase of the highest abundance $n = 3$ peak from $3.5 \times 10^6$ cps. (Figure 1) to $5.4 \times 10^7$ cps. (Figure 2). This highlights a crucial observation that default instrument parameters, tailored for ionization of large stable biomolecules, are often too harsh for preserving fragile assemblies such as coordination complexes.
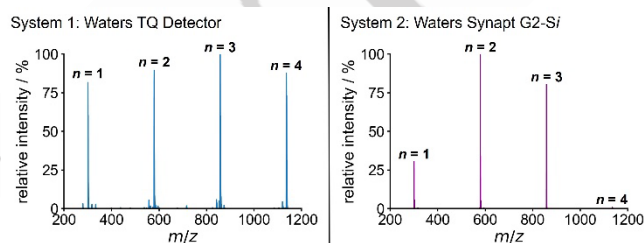


**Figure 2.** Positive-ion ESI mass spectra of $[Na(OPPh_3)_n]^+$ ions, where n = 1-4, for Systems 1 and 2, both collected at 80 °C source temperatures after automated optimization of MS parameters using OptiMS. The 100% relative intensity represents $5.4 \times 10^7$ cps. and $3.0 \times 10^9$ cps. absolute ion intensities for System 1 and 2, respectively.

As anticipated, higher cone voltages promote fragmentation, the degree of which depends on the voltage and the sample

composition, whereas the use of lower cone voltages can result in the observation of intact molecular ions.[33] There is a trade-off between reducing the voltages to minimize fragmentation and maintaining a good signal intensity with higher applied potentials. Thus, optimal conditions are expected to be different for each instrument. When weighing the trade-off, lower capillary voltages were additionally beneficial to avoid phenomena such as corona discharge, which can result in an unstable or lost MS signal.

This automated optimization approach not only improved signal stability and signal-to-noise (*S/N*) ratio, but also offered the potential to fine-tune these settings for different instruments, ensuring optimal performance in each unique scenario. For System 2, the optimized parameters, determined using OptiMS, enhanced the signal intensity of the $n = 4$ corresponding peak to $3.2 \times 10^7$ cps. above a baseline noise level of $5.1 \times 10^4$ cps. as shown in Figure 2. This compared to the initial non-optimized settings shown in Figure 1 corresponds to an increase in the *S/N* of two orders of magnitude. However, despite rigorous optimization attempts for System 2, no combination of parameter settings resulted in significantly large improvements in the absolute signal intensity of the tetrakis cation that matched the intensities of the $n = 1$-$3$ peaks, even with excess $OPPh_3$ present in solution. To address this challenge, further investigations were necessary to enhance the performance of System 2.

## Impact of source temperatures on ion fragmentation profiles

Using the positive-mode test, we investigated how the source temperature affected fragmentation in Systems 1 and 2 (Figure 3). The range of the instrument source temperature ramp was chosen to span the solvent boiling point (~80 °C in this case) and was ramped from 50-150 °C in 5 °C increments. Other instrument settings used in these tests were kept at the optimized parameters determined from the OptiMS optimization experiments.
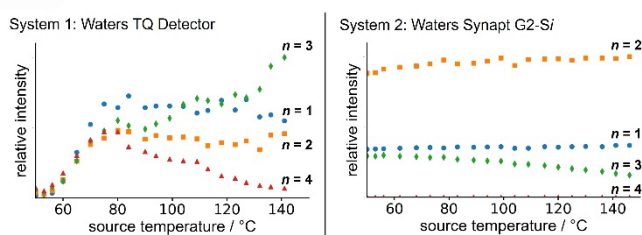


**Figure 3.** Normalized intensities of $[Na(OPPh_3)_n]^+$ ions, where n = 1-4, monitored during source temperature ramp (50-150 °C, 5 °C increments) obtained on Systems 1 and 2.

For System 1, raising the source temperature above 85 °C led to a reduction in the relative intensity of the $n = 4$ ion peak, mirrored by a concurrent increase in relative intensity of the fragmentation product $n = 3$ ion. This temperature-induced effect for System 1 is consistent with a known phenomenon in mass spectrometry, where excessive source temperatures promote fragmentation and denaturation.[45,46]

When we applied this temperature ramp to System 2, it became evident that detection of the $n = 4$ ion was virtually non-existent, even at low source temperatures. This very low abundance of high-coordinate ions further suggests that softness limitations in

# RESEARCH ARTICLE

System 2 are due to other aspects of instrument design, rather than in-source thermal ion fragmentation. As previously stated, it is postulated that fragmentation likely results from ions in the post-source region having a higher effective vibrational temperature.[38] This may be just one contributing factor among others such as the timescale of the experiment, trapping conditions, and auxiliary field parameters, leading to higher internal ion energy and increased ion fragmentation of high-coordinate ions.

Furthermore, the discrepancy in relative ion intensities for System 2 observed at variable temperatures (Figure 3) compared to at 80 °C source temperature (Figure 1b) may stem from experimental or instrumental variations. Despite efforts to maintain consistency, changes in instrument performance over time and data collection at different times could contribute to these differences. Additionally, slight variations in sample preparation, including $Na^+$ and $OPPh_3$ concentrations as shown in the SI (Figure S1), may lead to differences in the relative ion intensities observed.

These findings highlight the pivotal role of instrument design, specifications, and source parameter configurations in defining instrument softness. This temperature-dependent distribution of various species also underscores the challenges associated with sensitively detecting species with different thermal stabilities simultaneously. The often-slow response time of instruments to temperature changes practically impedes the seamless oscillation between analyte-specific temperatures within a single experiment, often necessitating compromises. To overcome this limitation, exploring alternative instrument configurations or adopting experimental strategies that enable more dynamic temperature control in response to the specific thermal stabilities of targeted ions may be essential.

## Comparative analysis of ESI-MS softness across multiple ESI-MS systems

Given the observed variability in results obtained from the two test instruments, we broadened our dataset through collaboration, using ESI-MS instruments from different manufacturers. Six additional instruments (Systems 3-8) were utilized, including two Sciex (Concorde, ON, Canada) QTRAP 5500 LC-MS/MS spectrometers equipped with a Sciex TurboSpray ion source (Systems 3 and 4); an Exactive Plus (ThermoFisher Scientific, MA) Orbitrap ESI-MS spectrometer (System 5) and a Q Exactive (ThermoFisher Scientific, MA) HF Hybrid Quadrupole-Orbitrap spectrometer (System 6), both equipped with an Ion Max API source with a HESI-II heated probe; a Bruker (Billerica, MA, USA) SolariX XR Fourier-Transform Ion Cyclotron Resonance (FT-ICR) spectrometer with 7T magnet equipped with a dual ESI/MALDI source (System 7); and an Agilent (Mississauga, Canada) 6545 LC/Q-Tof spectrometer with a Dual-AJS ion source (System 8). The ESI source conditions for these systems were chosen through manual parameter optimization aimed at maximizing the signal intensity of higher $n$ species, with additional experimental parameter configurations available in the SI Tables S3-8. This approach enabled us to amass a more comprehensive dataset, revealing significant variations in instrument softness.

Figure 4 displays mass spectra from six additional ESI-MS instruments, operating in positive ion mode, offering additional insights. Notably, these investigations revealed variability in signal intensity, particularly for the diagnostic $n$ = 4 ion peak. Consistent observation of the highest relative signal intensity for

the $n$ = 4 ion peak was found in both Systems 3 and 4. A comparative analysis of the two systems, both of which were Sciex QTRAP 5500 LC-MS/MS spectrometers, revealed congruent results, indicating reproducibility across different laboratories using identical instruments.

Nevertheless, variations were noted in the signal intensities, particularly with System 4 displaying reduced relative detections of the $n$ = 4 ion. Additionally, System 4 exhibited higher detection of the protonated species, evidenced by the dual peaks observed in the mass spectra, positioned at 21.98 Da lower than the expected sodiated peaks. These disparities suggest a nuanced influence of experimental parameters on the detection outcomes, with varied manual parameter optimization approaches used in the different labs. For instance, the elevated declustering potential applied in System 3, as summarized in the SI, may contribute to the breakdown of protonated species, lowering chemical noise and resulting in comparatively lower signal intensities.
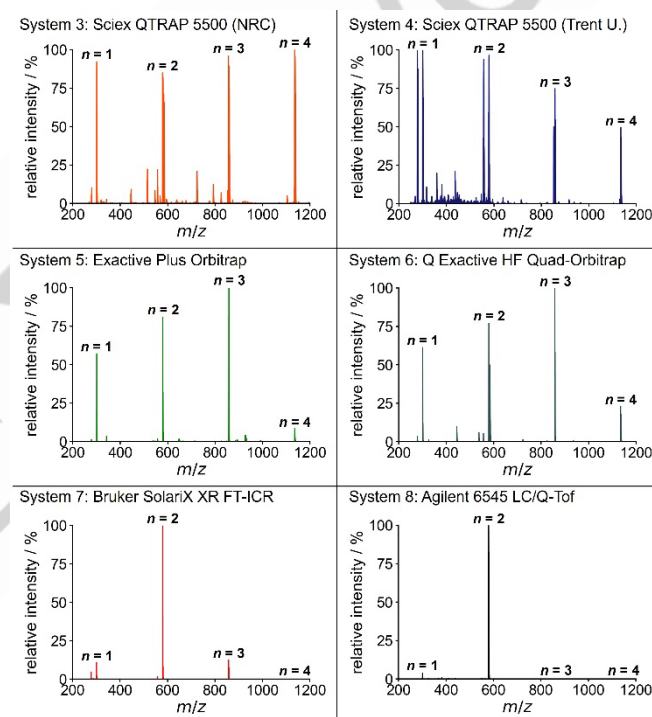


**Figure 4.** Positive-ion ESI mass spectra of $[Na(OPPh_3)_n]^+$ ions, where n = 1-4 collected on ESI-MS System 3-8, under varying manually optimized instrument parameters summarized in the SI Tables S3-8. Absolute ion intensities for the 100% relative intensity peak for Systems 3-8 are summarized in the SI Table S9.

System 5 and System 6 exhibited relatively modest signal intensities for the $n$ = 4 cation. Previous studies on optimizing source parameter for the HESI-II heated electrospray ionization interface used in these two systems have pinpointed the tube lens voltage and skimmer voltage as having the most pronounced impact on in-source fragmentation of the analyzed lipids.[10] Excessive heating and voltages applied can induce thermal effects, influencing the desolvation and activation of ions, leading to variations in both the types and extent of fragmentation observed in the mass spectra.[47] These fragmentation discrepancies may also be related to orbitrap instruments

# RESEARCH ARTICLE

applying strong fields to concentrate or trap ions in the C-trap prior to detection, potentially causing ion fragmentation within the mass analyzer.[48,49]

In contrast, Systems 7, detected only trace amounts of the four-coordinate [Na(OPPh$_3$)$_4$]$^+$ cation, with minimal signal above at the baseline. This FT-ICR MS operates on the principles of ion cyclotron resonance in a magnetic field, offering exceptional mass resolution, resolving power, and mass accuracy by trapping and analyzing ions.[50] However, the confinement of ions in the trap can result in the accumulation of internal energy through mechanisms such as ion-neutral collisions, RF excitation inducing oscillatory motion in ions causing energy deposition, and resonant excitation of ions at their cyclotron frequencies.[51]

Similar ion-trapping effects were observed in System 3, involving linear ion traps, where the $n$ = 3 signal intensity was significantly reduced due to an additional minimum 5 V trapping energy imparted (Figure S2). In this system, in addition to the pressure gradient that likely promotes energetic collisional activation, the coupling of radial and axial ion motion near the trap exit can result in ions receiving a proportionately higher kinetic energy boost, potentially leading to instability and fragmentation from collisions.[52] While the exact reason for the higher energy levels in the trapping modes of the QTRAP is not definitively established, this characteristic is specific to that particular instrument rather than a general feature of ion trap mass analyzers, which are not inherently less soft.

In System 8, no substantial amounts of the four-coordinate cation were detected. In this system, excess energy is likely imparted on ions through the use of the Agilent Jet Stream (AJS) thermal gradient focusing technology, involving a superheated nitrogen sheath gas introduced collinear with the pneumatically assisted electrospray.[53]

In the negative ion mode, some analogous patterns were noted compared to the positive ion mode, albeit with a more limited set of instruments as shown in Figure 5. It is noteworthy that the relative abundance of the $n$ = 2 species displayed variations among the instruments, further shedding light on the divergent softness of the tested systems. Additionally, sample preparation also played a significant role in these tests.
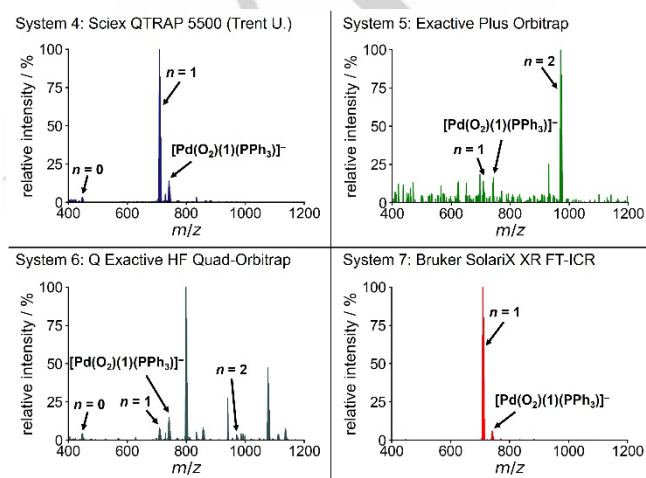


**Figure 5.** Negative-ion ESI mass spectra of [Pd(**1**)(PPh$_3$)$_n$]$^-$ ions, where n = 0-2, collected on ESI-MS Systems 4-7, under varying manually optimized

instrument parameters summarized in the SI Tables S3-8. Absolute ion intensities for the 100% relative intensity peak for Systems 3-8 are summarized in the SI Table S9.

For System 5, where a Schlenk line was used in sample preparation, a high relative intensity of the $n$ = 2 species was observed, however, significant chemical background was observed in this case. Systems 4 and 7, lacking access to a Schlenk line or glovebox, utilized degassed solvent and a quick "dump and mix" to minimize oxidation. Despite these efforts, some oxidation was observed as evidenced by the detection of dioxygenated palladium species [Pd(O$_2$)(**1**)(PPh$_3$)]$^-$ ($m/z$ 741.0251), along with minimal detection of the $n$ = 2 species. In the case of System 6, the absence of an inert glovebox or Schlenk line likely led to increased oxidation. Moreover, other adducts and decomposition products were also identified in this system. These observations highlight the necessity of considering the availability of inert atmospheres during experimental design, and the impact of sample handling conditions on the detection outcomes and interpretation.

## Evaluating sample handling techniques in negative ion mode

When performing the negative ion mode test, a notable additional feature is the experiment's capability to detect O$_2$ exclusion. Maintaining moisture- and air-free conditions can have a significant impact on the reactivity and reproducibility of organometallic reactions.[54] In this context, this test provides additional utility and is particularly beneficial for trainees, offering insight into the effectiveness of air-sensitive sample handling techniques. We have previously shown the rapid catalytic oxidation of triphenylphosphine via Pd(PPh$_3$)$_4$ in the presence of O$_2$ in solution.[55] As such, this experiment serves as a test for O$_2$ concentration with the detection of the phosphine oxide ion [**1**+O]$^-$ ($m/z$ 357.0356) disclosing the degree of O$_2$ contamination.
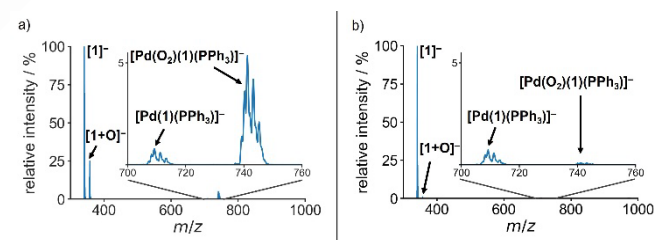


**Figure 6.** Negative-ion ESI mass spectra obtained for System 1 showing relative amounts of phosphine [**1**]$^-$ ($m/z$ 341.0407) and phosphine oxide [**1**+O]$^-$ ($m/z$ 357.0356) resulting from; a) poor O$_2$-free handling techniques, and b) O$_2$ exclusion by solvent degassing. Insets show low abundant species [Pd(**1**)(PPh$_3$)]$^-$ ($m/z$ 709.0353) and [Pd(O$_2$)(**1**)(PPh$_3$)]$^-$ ($m/z$ 741.0251) amplified ×20. The 100% relative intensity represents 9.1 × 10$^6$ cps. and 1.4 × 10$^7$ cps. absolute ion intensities for (a) and (b), respectively.

A comparison of poor and good sample handling techniques is shown in Figure 6. Figure 6a depicts the results of sample preparation in which solvent was collected directly from the solvent bottle without the use of any degassing procedures. This resulted in a phosphine-to-phosphine oxide signal intensity ratio of 1:0.26, as well as the detection of the dioxygenated palladium

## RESEARCH ARTICLE

species $[Pd(O_2)(\mathbf{1})(PPh_3)_n]^-$ ($m/z$ 741.0251) in appreciable amounts.[55] When oxygen is excluded by a freeze-pump-thaw cycle and suitable Schlenk line techniques, the intensity ratio of $PPh_3$ to $OPPh_3$ is reduced to 1:0.02, along with the minimal dioxygenated palladium species (Figure 6b). As such, the intensity of $OPPh_3$ indicates the presence of $O_2$ in an inert atmosphere, though such conditions are common in many catalytic reactions.

## Conclusion

This study demonstrates the importance of assessing the softness of ESI-MS systems used in detecting easily fragmented species, such as coordination complexes and organometallic compounds. By employing a set of tests for a quick relative assessment of softness specific to weakly coordinating organometallic and coordination species, our findings reveal significant variations in instrument softness, even among instruments from the same manufacturer. These tests highlight the importance of selecting appropriate instrumentation and carefully controlling instrument energetics, such as trapping conditions and auxiliary field parameters where possible, to minimize excess ion energy and fragmentation. Equally significant, our observations reveal that even after optimization, certain systems exhibit varying degrees of suitability for detecting fragile species. This underscores the need for a nuanced understanding of instrument capabilities in the context of specific analytes and application.

Additionally, we identified a system that can serve as a useful probe for sample handling quality, such as the exclusion of $O_2$. It is worth emphasizing that while our study provides a relative comparative assessment of ESI-MS softness, it does not cover all available instruments comprehensively. However, these results can serve as a valuable guide for users making crucial decisions regarding the suitability of an instrument for their specific research needs. We recommend that MS users consider these limitations and conduct tests similar to those proposed in this work to determine the optimal conditions for their instrument and sample composition.

## Experimental Section

### Positive-mode ESI-MS of $[Na(OPPh_3)_n]^+$

In a typical experiment, aliquots of a NaCl solution (1.0 mM in $H_2O$, 0.1 mL, 0.1 μmol) and a triphenylphoshine oxide ($OPPh_3$) solution (1.0 mM in MeOH, 0.4 mL, 0.1 μmol) were mixed, and the sample made up to 2 mL with methanol (MeOH) to form a 1:4 equivalent sample (0.05 mM NaCl and 0.20 mM $OPPh_3$). Infusion of the sample into a mass spectrometer yielded a spectrum of $[Na(OPPh_3)_n]^+$, where $n$ = 1-4, with expected peaks at $m/z$ 301.0753, 579.1613, 875.2474, and 1135.3334 for $n$ = 1-4, respectively.

### Negative-mode ESI-MS of $[Pd(\mathbf{1})(PPh_3)_n]^-$

An equimolar solution of 0.5 mM bis(triphenylphosphine)iminium triphenylphosphine monosulfonate $[PPN]^+[P(Ph)_2(m\text{-}C_6H_4SO_3)]^-$ or $[PPN][\mathbf{1}]$[42,56] and 0.5 mM $Pd(PPh_3)_4$ was prepared in 9:1

MeOH/tetrahydrofuran (THF). The solution was prepared using standard Schlenk line techniques,[57] and kept under inert atmosphere where available. A 1 mL sample of the solution was collected, with infusion into a mass spectrometer yielding a spectrum of $[Pd(\mathbf{1})(PPh_3)_n]^-$, where $n$ = 0-2, with expected peaks at $m/z$ 446.9442, 709.0353, and 971.1264 for $n$ = 0-2, respectively.

## Supporting Information

The Supporting Information for this article is available via the link provided. This document includes:
materials and chemicals used; ESI-MS instruments operating parameters (Tables S8); absolute ion intensities (Table S9); general test procedures; stoichiometric effects on $[Na(OPPh3)_n]^+$ spectra (Figure S1); fragmentation by ion trapping for System 3 (Figure S2).

## Author Contributions

The project was conceptualized by ICC and JSM. Methodology was developed by ICC, TF, and JSM. Investigations were carried out by ICC, PJHW, TF, NLS, DGB, GTT, and JZ. Visualizations by ICC. Writing (original draft) by ICC, (review & editing) by ICC, PJHW, NLS, DGB, and JSM. Supervision by JSM.
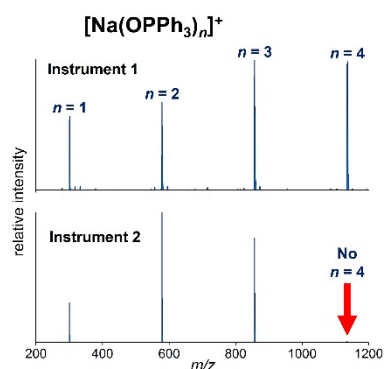
## Acknowledgements

[1] G.-J. Cheng, X.-M. Zhong, Y.-D. Wu, X. Zhang, *Chem. Commun.* **2019**, *55*, 12749–12764.
[2] J. C. Traeger, *Int. J. Mass Spectrom.* **2000**, *200*, 387–401.
[3] C. C. Oliveira, M. V. Marques, M. N. Godoi, T. Regiani, V. G. Santos, E. A. F. dos Santos, M. N. Eberlin, M. M. Sá, C. R. D. Correia, *Org. Lett.* **2014**, *16*, 5180–5183.
[4] A. A. Sabino, A. H. L. Machado, C. R. D. Correia, M. N. Eberlin, *Angew. Chem.* **2004**, *116*, 2568–2572.
[5] M. Deuker, Y. Yang, R. A. J. O'Hair, K. Koszinowski, *Organometallics* **2021**, *40*, 2354–2363.
[6] R. Chung, D. Yu, V. T. Thai, A. F. Jones, G. K. Veits, J. Read de AAniz, J. E. Hein, *ACS Catal.* **2015**, *5*, 4579–4585.
[7] D. Schröder, *Acc. Chem. Res.* **2012**, *45*, 1521–1532.
[8] L. Konermann, H. Metwally, Q. Duez, I. Peters, *Analyst* **2019**, *144*, 6157–6171.
[9] P. Kebarle, *J. Mass Spectrom.* **2000**, *35*, 804–817.
[10] R. M. Gathungu, P. Larrea, M. J. Sniatynski, V. R. Marur, J. A. Bowden, J. P. Koelmel, P. Starke-Reed, V. S. Hubbard, B. S. Kristal, *Anal. Chem.* **2018**, *90*, 13523–13532.
[11] V. Gabelica, E. D. Pauw, *Mass Spectrom. Rev.* **2005**, *24*, 566–587.
[12] T. Nishimura, in *Fundam. Mass Spectrom.* (Ed.: K. Hiraoka), Springer, New York, NY, **2013**, pp. 29–54.

[13] J. H. Gross, in *Mass Spectrom. Textb.* (Ed.: J.H. Gross), Springer International Publishing, Cham, **2017**, pp. 721–778.

[14] J. M. Hayes, G. J. Small, *Anal. Chem.* **1983**, *55*, 565A–574A.

[15] J. T. Davidson, Z. J. Sasiene, G. P. Jackson, *J. Mass Spectrom.* **2021**, *56*, e4679.

[16] C. Markert, M. Thinius, L. Lehmann, C. Heintz, F. Stappert, W. Wissdorf, H. Kersten, T. Benter, B. B. Schneider, T. R. Covey, *Anal. Bioanal. Chem.* **2021**, *413*, 5587–5600.

[17] G. Rovelli, M. I. Jacobs, M. D. Willis, R. J. Rapf, A. M. Prophet, K. R. Wilson, *Chem. Sci.* **2020**, *11*, 13026–13043.

[18] M. A. Raji, K. A. Schug, *Int. J. Mass Spectrom.* **2009**, *279*, 100–106.

[19] J. S. Page, R. T. Kelly, K. Tang, R. D. Smith, *J. Am. Soc. Mass Spectrom.* **2007**, *18*, 1582–1590.

[20] J. Liigand, A. Kruve, P. Liigand, A. Laaniste, M. Girod, R. Antoine, I. Leito, *J. Am. Soc. Mass Spectrom.* **2015**, *26*, 1923–1930.

[21] J. T. Cox, I. Marginean, R. D. Smith, K. Tang, *J. Am. Soc. Mass Spectrom.* **2015**, *26*, 55–62.

[22] Y. Kang, B. B. Schneider, L. Bedford, T. R. Covey, *J. Am. Soc. Mass Spectrom.* **2019**, *30*, 2347–2357.

[23] J. Kaeslin, C. Wüthrich, S. Giannoukos, R. Zenobi, *J. Am. Soc. Mass Spectrom.* **2022**, *33*, 1967–1974.

[24] R. Rahrt, T. Auth, M. Demireva, P. B. Armentrout, K. Koszinowski, *Anal. Chem.* **2019**, *91*, 11703–11711.

[25] R. G. Belli, Y. Wu, H. Ji, A. Joshi, L. P. E. Yunker, J. S. McIndoe, L. Rosenberg, *Inorg. Chem.* **2019**, *58*, 747–755.

[26] G. T. Thomas, E. Janusson, H. S. Zijlstra, J. S. McIndoe, *Chem. Commun.* **2019**, *55*, 11727–11730.

[27] A. Joshi, H. S. Zijlstra, S. Collins, J. S. McIndoe, *ACS Catal.* **2020**, *10*, 7195–7206.

[28] D. Asakawa, R. Yamamoto, N. Hanari, K. Saikusa, *Anal. Methods* **2023**, *15*, 6150–6158.

[29] W. Henderson, J. S. McIndoe, *Mass Spectrometry of Inorganic and Organometallic Compounds*, John Wiley & Sons, Ltd., New York, **2005**.

[30] A. Kruve, K. Kaupmees, J. Liigand, M. Oss, I. Leito, *J. Mass Spectrom.* **2013**, *48*, 695–702.

[31] A. Kruve, K. Kaupmees, *J. Am. Soc. Mass Spectrom.* **2017**, *28*, 887–894.

[32] Z. S. Breitbach, E. Wanigasekara, E. Dodbiba, K. A. Schug, D. W. Armstrong, *Anal. Chem.* **2010**, *82*, 9066–9073.

[33] L. S. Bonnington, R. K. Coll, E. J. Gray, J. I. Flett, W. Henderson, *Inorganica Chim. Acta* **1999**, *290*, 213–221.

[34] P. J. H. Williams, I. C. Chagunda, J. S. McIndoe, *J. Am. Soc. Mass Spectrom.* **2024**, *35*, 449–455.

[35] W. Corporation, *Waters TQ Detector Operator's Guide*, Waters Corporation, Milford, USA, **2015**.

[36] W. Corporation, *SYNAPT G2-Si HDMS Mass Spectrometer Overview and Maintenance Guide*, Waters Corporation, Milford, USA, **2016**.

[37] J. H. Gross, in *Mass Spectrom. Textb.* (Ed.: J.H. Gross), Springer International Publishing, Cham, **2017**, pp. 539–612.

[38] D. Morsa, E. Hanozin, G. Eppe, L. Quinton, V. Gabelica, E. D. Pauw, *Anal. Chem.* **2020**, *92*, 4573–4582.

[39] J. Sherwood, J. H. Clark, I. J. S. Fairlamb, J. M. Slattery, *Green Chem.* **2019**, *21*, 2164–2213.

[40] M. Paul, K. Laketic, J. S. McIndoe, *Can. J. Chem.* **2021**, *99*, 87–92.

[41] M. Y. C. Ting, L. P. E. Yunker, I. C. Chagunda, K. Hatlelid, M. Vieweg, J. S. McIndoe, *Catal. Sci. Technol.* **2021**, *11*, 4406–4416.

[42] K. L. Vikse, M. A. Henderson, A. G. Oliver, J. S. McIndoe, *Chem. Commun.* **2010**, *46*, 7412–7414.

[43] P. Vidossich, G. Ujaque, A. Lledós, *Chem. Commun.* **2013**, *50*, 661–663.

[44] D. P. Elpa, G. R. D. Prabhu, S.-P. Wu, K. S. Tay, P. L. Urban, *Talanta* **2020**, *208*, 120304.

[45] A. L. Rockwood, M. Busman, H. R. Udseth, R. D. Smith, *Rapid Commun. Mass Spectrom.* **1991**, *5*, 582–585.

[46] J. Alexander Harrison, A. Pruška, I. Oganesyan, P. Bittner, R. Zenobi, *Chem. – Eur. J.* **2021**, *27*, 18015–18028.

[47] L. Bernier, H. Pinfold, M. Pauly, S. Rauschenbach, J. Reiss, *J. Am. Soc. Mass Spectrom.* **2018**, *29*, 761–773.

[48] R. A. Zubarev, A. Makarov, *Anal. Chem.* **2013**, *85*, 5288–5296.

[49] E. S. Hecht, M. Scigelova, S. Eliuk, A. Makarov, in *Encycl. Anal. Chem.*, John Wiley & Sons, Ltd, **2019**, pp. 1–40.

[50] M. Tiquet, R. La Rocca, S. Kirnbauer, S. Zoratto, D. Van Kruining, L. Quinton, G. Eppe, P. Martinez-Martinez, M. Marchetti-Deschmann, E. De Pauw, J. Far, *Anal. Chem.* **2022**, *94*, 9316–9326.

[51] A. G. Marshall, *Int. J. Mass Spectrom.* **2000**, *200*, 331–356.

[52] J. W. Hager, *Rapid Commun. Mass Spectrom.* **2002**, *16*, 512–526.

[53] H. Wasito, T. Causon, S. Hann, *Talanta* **2022**, *236*, 122828.

[54] A. Joshi, C. Killeen, T. Thiessen, H. S. Zijlstra, J. S. McIndoe, *J. Mass Spectrom.* **2022**, *57*, DOI 10.1002/jms.4807.

[55] A. V. Hesketh, S. Nowicki, K. Baxter, R. L. Stoddard, J. S. McIndoe, *Organometallics* **2015**, *34*, 3816–3819.

[56] M. R. Barton, Y. Zhang, J. D. Atwood, *J. Coord. Chem.* **2002**, *55*, 969–983.

[57] A. M. Borys, *Organometallics* **2023**, *42*, 182–196.

## RESEARCH ARTICLE

## Entry for the Table of Contents



$[Na(OPPh_3)_n]^+$

Instrument 1
n = 1
n = 2
n = 3
n = 4

Instrument 2
No n = 4

relative intensity

m/z

This study investigates the soft ionization process of electrospray ionization mass spectrometry (ESI-MS) and its implication for detecting thermally fragile inorganic species. It presents simple tests that reveal notable variations in instrument softness, highlighting the importance of instrument parameter optimization. These findings offer valuable guidance for selecting suitable instrument systems for a given analysis and ensuring dependable results.